HHS Public Access

Author manuscript

Cell Rep. Author manuscript; available in PMC 2018 March 27.

Published in final edited form as:

Cell Rep. 2018 March 13; 22(11): 2995–3005. doi:10.1016/j.celrep.2018.02.076.

Clinical and Genomic Crosstalk between Glucocorticoid Receptor and Estrogen Receptor α In Endometrial Cancer

Jeffery M. Vahrenkamp[1,2], **Chieh-Hsiang Yang**[3,4], **Adriana C. Rodriguez**[1,2], **Aliyah Almomen**[3,5], **Kristofer C. Berrett**[1,2], **Alexis N. Trujillo**[6], **Katrin P. Guillen**[1,2], **Bryan E. Welm**[1,2,7], **Elke A. Jarboe**[2,8], **Margit M. Janat-Amsbury**[3,4,9], and **Jason Gertz**[1,2,10,*]

[1]Department of Oncological Sciences, University of Utah, Salt Lake City, UT 84112, USA

[2]Huntsman Cancer Institute, University of Utah, Salt Lake City, UT 84112, USA

[3]Division of Gynecologic Oncology, Department of Obstetrics and Gynecology, University of Utah, Salt Lake City, UT 84112, USA

[4]Department of Bioengineering, University of Utah, Salt Lake City, UT 84112, USA

[5]College of Pharmacy, King Saud University, Riyadh, Kingdom of Saudi Arabia

[6]University of New Mexico, Albuquerque, NM 87131, USA

[7]Department of Surgery, University of Utah, Salt Lake City, UT 84112, USA

[8]Department of Pathology, University of Utah, Salt Lake City, UT 84112, USA

[9]Department of Pharmaceutics and Pharmaceutical Chemistry, University of Utah, Salt Lake City, UT 84112, USA

SUMMARY

Steroid hormone receptors are simultaneously active in many tissues and are capable of altering each other's function. Estrogen receptor α (ER) and glucocorticoid receptor (GR) are expressed in the uterus, and their ligands have opposing effects on uterine growth. In endometrial tumors with high ER expression, we surprisingly found that expression of GR is associated with poor prognosis. Dexamethasone reduced normal uterine growth *in vivo*; however, this growth inhibition was abolished in estrogen-induced endometrial hyperplasia. We observed low genomic-binding

*Correspondence: jay.gertz@hci.utah.edu.
10Lead Contact

AUTHOR CONTRIBUTIONS

Conceptualization, J.M.V., M.M.J.-A., and J.G.; Investigation, J.M.V., C.-H.Y., A.C.R., A.A., K.C.B., A.N.T., K.P.G., and E.A.J; Supervision, B.E.W., E.A.J., M.M.J.-A., and J.G.; Writing – Original Draft, J.M.V., A.C.R., and J.G.; Writing – Review & Editing, all authors; Funding Acquisition, J.G.

DATA AND SOFTWARE AVAILABILITY

The accession number for the ChIP-seq, RNA-seq, and ATAC-seq data (along with alignments, peak calls, and gene read counts) reported in this paper is GEO: GSE109893.

SUPPLEMENTAL INFORMATION

Supplemental Information includes seven figures and can be found with this article online at https://doi.org/10.1016/j.celrep.2018.02.076.

DECLARATION OF INTERESTS

The authors declare no competing interests.

site overlap when ER and GR are induced with their respective ligands; however, upon simultaneous induction they co-occupy more sites. GR binding is altered significantly by estradiol with GR recruited to ER-bound loci that become more accessible upon estradiol induction. Gene expression responses to co-treatment were more similar to estradiol but with additional regulated genes. Our results suggest phenotypic and molecular interplay between ER and GR in endometrial cancer.

Graphical abstract

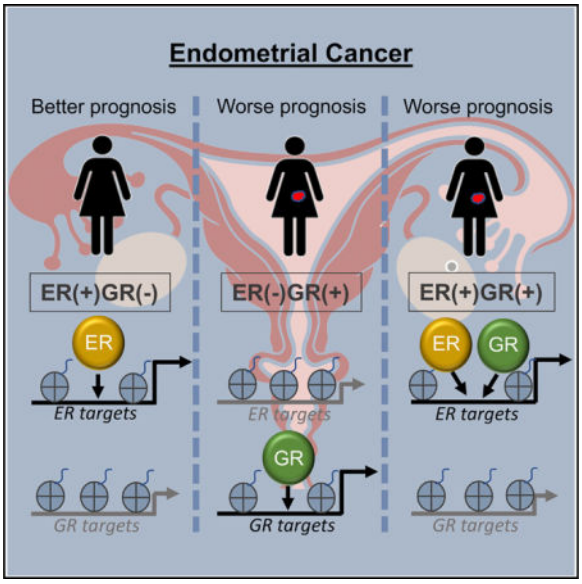

INTRODUCTION

Steroid hormone receptors have similar DNA-binding preferences, and their genomic binding is dependent on an overlapping set of additional transcription factors (Jozwik and Carroll, 2012; Robinson et al., 2011). Therefore, it is not surprising that the actions of one steroid hormone receptor can be altered by the induction of a different steroid hormone receptor. For example, progesterone receptor (PR) and estrogen receptor α (ER) often are co-expressed in breast cancer, and the induction of PR redirects ER genomic binding and reduces estrogen-driven growth (Mohammed et al., 2015; Singhal et al., 2016). Androgens enable breast cancer growth, and androgen receptor (AR) is important for ER genomic binding (D'Amato et al., 2016). Steroid hormones also are capable of compensating for one another. In prostate cancer, dexamethasone can confer resistance to anti-androgen therapy by activating glucocorticoid receptor (GR), which can substitute for AR in regulating transcription (Arora et al., 2013; Isikbay et al., 2014; Li et al., 2017). In the luminal androgen receptor subtype of breast cancer, AR compensates for the absence of ER by binding to similar genomic loci that are occupied by FOXA1 (Robinson et al., 2011). It is clear that steroid hormone receptors do not work in isolation and that they can perform overlapping functions.

GR and ER have been shown to alter each other's regulatory and phenotypic roles. GR expression is associated with good outcomes in ER-positive breast cancer and poor outcomes in ER-negative breast cancer (Pan et al., 2011), which is consistent with dexamethasone-blocking estrogen-induced growth in breast cancer cells (Zhou et al., 1989). When both steroid hormone receptors are active in breast cancer cells, GR affects the genomic interactions of ER (Miranda et al., 2013). GR activation alters chromatin accessibility, enabling ER to bind to a new set of genomic regions, a mechanism known as assisted loading (Voss et al., 2011). In addition, ER and GR have been shown to both cooperate with (Bolt et al., 2013) and compete (Karmakar et al., 2013; Meyer et al., 1989) for co-factors in breast cancer cells. GR also has been implicated in *trans*-repression of ER-regulated gene expression in breast cancer (Yang et al., 2017). Estrogens and corticosteroids can elicit opposite phenotypic effects in other tissues as well (Haynes et al., 2003; Lam et al., 1996; Terakawa et al., 1985), including the uterus (Gunin et al., 2001; Markaverich et al., 1981; Rabin et al., 1990; Rhen et al., 2003).

Endometrial cancer is the most common gynecological cancer. Incidence, as well as mortality, associated with endometrial cancer is on the rise, and survival rates are significantly worse now than in the 1970s. Of endometrial cancers, 80%–90% are type I endometrioid tumors that express ER and are thought to be hormonally driven (Saso et al., 2011). Estrogen causes increased uterine growth and continued exposure can lead to endometrial hyperplasia (Yang et al., 2015). In contrast to the pro-growth role of ER in the uterus, GR reduces uterine growth and opposes phenotypic effects of estrogens in the uterus (Bever et al., 1956; Bitman and Cecil, 1967). Despite the opposing phenotypic roles, dexamethasone (Dex) and 17β-estradiol (E2), a GR and an ER agonist, respectively, produce similar gene expression changes in the normal uterus (Rhen et al., 2003). Although estrogen and corticosteroid signaling have been examined in the normal uterus, crosstalk between ER and GR has not been explored in the context of endometrial cancer on a genome-wide scale.

Here, we show that GR expression is associated with poor prognosis and higher grade in endometrioid endometrial cancers, which is unexpected considering the growth-inhibitory effects of corticosteroids in the normal uterus. Consistent with this observation, we find that once E2-induced hyperplasia is established in mice, growth is no longer opposed by Dex. Analysis of GR and ER genomic binding in endometrial cancer cells uncovered an interesting relationship in which E2, in combination with Dex, enables GR to bind to an expanded repertoire of genomic loci. Based on chromatin-accessibility patterns, ER appears to assist in chromatin loading of GR. Gene-expression analysis indicates that double induction with E2 and Dex produces a response similar to the addition of the separate inductions; however, several genes are affected by the double treatment in a nonlinear manner. Taken together, our results indicate that ER affects the gene regulatory and phenotypic actions of GR in endometrial cancer cells and that GR activity may lead to more aggressive forms of the disease.

RESULTS

Glucocorticoid Receptor Expression Is Associated with Poor Prognosis in Endometrial Cancer

Because steroid hormone receptors can affect one another's phenotypic and gene regulatory outputs, we decided to look for an association between gene expression of steroid hormone receptors and outcomes in endometrioid endometrial cancer, a hormonally driven type of cancer. We focused our analysis on endometrial cancer RNA-seq and clinical data from The Cancer Genome Atlas (TCGA) (Kandoth et al., 2013), exclusively analyzing tumors with endometrioid histology. Although ER is expressed at the mRNA level in most tumors, higher expression is associated with longer disease-free survival (Figure 1A; $p = 0.002791$, Cox regression), which is consistent with previous reports for ER protein and mRNA levels (Wik et al., 2013). Higher ER expression also was associated with lower grade (Figure 1D, $p = 1.75 \times 10^{-7}$, Wilcoxon), as previously observed with ER protein levels (Backes et al., 2016), indicating that ER expression is higher in more differentiated tumors. PR is transcriptionally regulated by ER, and therefore it is not surprising that higher expression of PR is associated with better outcomes (Figure S1; $p = 0.0006479$, Cox regression), as previously reported (Tangen et al., 2014). Expression of AR, mineralocorticoid receptor, and estrogen receptor b were not significantly associated with recurrence (Figure S1).

Higher GR expression was associated with worse outcomes for patients with endometrioid endometrial tumors (Figure 1B, $p = 0.012$, hazard ratio = 2.1, Cox regression). Higher expression also was correlated with higher histological grade (Figure 1E; $p = 0.04$, Wilcoxon). To assess protein expression and GR activity in endometrioid tumors, we performed immunohistochemistry (IHC) and found that 27% (3/11) of grade 1 endometrioid tumors exhibited nuclear GR staining, which is indicative of active GR, and 50% (5/10) of grade 3 endometrioid tumors were positive for nuclear GR staining (examples in Figures 1F and S2). IHC confirms that GR is expressed and active in endometrial cancer cells and is more likely to be present in higher-grade endometrioid endometrial tumors.

To explore further the relation between GR expression and poor prognosis, we analyzed this association in the higher ER-expressing tumors and the lower ER-expressing tumors separately. Figure 1C shows that association between GR expression and disease-free survival is seen only in the tumors with higher ER expression ($p = 0.0096$, hazard ratio = 3 [95% confidence interval 1.3–7.3], Cox regression) and not observed in the tumors with lower ER expression ($p = 0.94$, hazard ratio = 0.97 [95% confidence interval 0.42–2.23], Cox regression). These results suggest that GR expression increases the aggressiveness of tumors with higher expression of ER, but it has little effect on tumors with low ER expression, indicating that ER and GR could be affecting the actions of each other.

E2 and Dex in Combination Induce Growth of Endometrial Cancer Cells in 3D Culture

Positive correlation between GR expression and the likelihood of recurrence is surprising and appears inconsistent in light of multiple studies connecting GR activation with reduced uterine growth (Gunin et al., 2001; Markaverich et al., 1981; Rabin et al., 1990; Rhen et al., 2003). We hypothesized that the growth-inhibitory effects of corticosteroids may be absent

once hyperplasia is established. We first evaluated how ER and GR affect endometrial cancer cell growth *in vitro*. The endometrial cancer cell line Ishikawa was grown in 3D Matrigel (Corning) culture in the presence of hormone-depleted media and then treated with E2, Dex, or their combination for 14 days. We then measured ATP levels and observed an expected loss of cell growth in hormone-depleted media (Figure 2A). The addition of E2 and Dex individually had subtle and insignificant effects on proliferation. However, when organoids were treated with both E2 and Dex, there was a significant increase in growth that came close to full media levels. This evidence indicates that ER and GR work together in promoting the growth of endometrial cancer cells.

Dex Inhibition of Uterine Growth Is Not Observed once Estrogen-Driven Hyperplasia Is Established

We next sought to determine the impact of active ER and GR on endometrial cells *in vivo*. We used an estrogen-induced endometrial hyperplasia model that uses a slow-release E2 pellet (Yang et al., 2015). We found that 3 weeks of Dex treatment, in the absence of excess E2, reduced uterine weight by 21% ($p = 0.042$, t test), whereas 10 weeks of E2 exposure increased uterine weight by 52% ($p = 0.002$, t test) (Figures 2B and 2C). When we administered Dex after allowing hyperplasia to establish during 10 weeks of excess E2, we found that Dex was unable to significantly inhibit uterine growth ($p = 0.24$, t test; 7.8% decrease) (Figures 2B and 2C). Histopathological review of H&E-stained slides from harvested and processed uteri revealed that endometrial hyperplasia persisted in five of six mice treated with Dex after E2, as compared to seven of seven mice treated with only E2. We observed the largest effects on endometrium growth, which is significantly thicker after E2 treatment (Figure S3; $p = 6.7 \times 10^{-6}$, Wilcoxon), whereas myometrium growth is slightly reduced by E2 ($p = 0.0179$, Wilcoxon). Overall, these results suggest that the inhibitory effect of GR on uterine growth is reduced significantly once hyperplasia is established.

GR Binds Loci Occupied by ER upon E2 and Dex Treatment

Survival analysis and phenotypic observations suggest that ER and GR may affect each other's roles. To determine how this crosstalk is occurring at a molecular level, we performed chromatin immunoprecipitation sequencing (ChIP-seq) with antibodies targeting ER and GR in Ishikawa, a human endometrial adenocarcinoma cell line. We found that ER and GR, when induced by E2 and Dex, respectively, have mostly unique binding profiles, with only 19.7% of GR-bound loci overlapping ER-bound loci. However, when cells are treated with E2 and Dex simultaneously, GR and ER share almost half of their binding sites (46.5%). This co-occurrence in ER and GR binding upon the double induction represents a significant increase compared to ER and GR after single inductions ($p < 2.2 \times 10^{-16}$, odds ratio = 3.96, Fisher's exact test; all overlaps shown in Figure S4A). These findings indicate that ER and GR affect each other on the genomic binding site selection level.

Further analysis of the ER- and GR-bound sites following double induction revealed that GR is moving to sites that are bound by ER. The majority (91.8%) of ER-bound sites in the double induction were bound by ER in cells treated with E2 alone (Figure 3A), and the sites unique to the double induction appear to be accompanied by small changes in the ChIP-seq signal (Figure 3B). In contrast, 63.1% of GR-bound sites in the double induction were bound

by GR in cells treated only with Dex, and the sites unique to the double induction exhibit large changes in ChIP-seq signal (Figure 3C). Of the 598 sites that were bound by GR only in the double induction, 67.5% overlapped with ER, suggesting that most of the new GR-binding sites in the double induction are loci that are bound by ER after both E2 and E2 + Dex treatments. The presence of estrogen-response elements (EREs) and glucocorticoid receptor-binding elements (GRBEs) are consistent with this idea; we found that loci bound by GR only after the double induction are enriched for both full- and half-site EREs compared to GRBEs (Table 1). The increase in GR genomic binding is not the result of increased expression because GR mRNA and protein levels are unaffected by the treatments (Figures S4B and S4C). Overall, these results indicate that ER is enabling GR to bind new genomic loci when both steroid hormone receptors are active.

Histone Acetylation Is Increased by E2 and Dex Co-treatment at Sites Bound by ER and GR

To determine whether binding of ER and GR to genomic loci upon double induction affected the regulatory activity of these regions, we analyzed acetylation of histone H3 lysine 27 (H3K27ac), a mark associated with active regulatory regions. We performed ChIP-seq, with an antibody that recognizes H3K27ac, on cells that were treated with Dex, E2, the combination of Dex and E2, or DMSO (vehicle control) for 8 hr. We found that at GR sites bound in the Dex-only treatment, there were no significant changes in H3K27ac after any treatment in comparison to vehicle (Figure 4A; $p > 0.01$, Wilcoxon). Sites bound by ER after E2-only treatment exhibited higher levels of H3K27ac after E2 treatment and the combination treatment compared to vehicle (Figure 4B; $p < 2.2 \times 10^{-16}$, Wilcoxon). Genomic loci that are bound by both GR and ER following the combination treatment had significantly higher levels of H3K27ac after the combination treatment compared to vehicle, E2 alone, and Dex alone (Figure 4C; $p = 2.3 \times 10^{-5}$, Wilcoxon). The pattern of H3K27ac enrichment at loci bound by both ER and GR indicates that binding of ER and GR to the same locus leads to molecular changes that are not observed when only one factor is active.

Chromatin Accessibility Patterns Are Consistent with ER Assisting GR in Chromatin Loading

One potential explanation for ER enabling GR genomic binding is assisted loading, in which one transcription factor makes it easier for another factor to bind by increasing accessibility to the genomic site (Voss et al., 2011). This phenomenon has been observed in breast cancer cells, although in the opposite direction, with GR enabling ER binding (Miranda et al., 2013). To test this model, we performed assay for transposase-accessible chromatin using sequencing (ATAC-seq) on Ishikawa cells treated with Dex, E2, or vehicle controls for 1 hr. We focused our analysis first on loci that were bound by GR either after induction with Dex or only after induction with both E2 and Dex. The loci bound only after the double induction exhibited significantly higher E2-induced chromatin accessibility as measured by ATAC-seq (Figure 5A; $p < 2.2 \times 10^{-16}$, Wilcoxon). This result is consistent with ER creating a more permissive binding environment for GR, enabling GR to bind only after the double induction. Figure 5C and 5D show example loci bound by GR only after double induction that also become more accessible upon E2 induction. In total, 65% of loci bound by GR only after the double induction exhibit increased accessibility after E2 treatment, compared to 43% of all GR-bound loci. We performed a similar analysis for loci bound by ER only after

double induction and found that chromatin accessibility increases significantly upon Dex induction (Figure 5B; p = 0.0001223, Wilcoxon), but the effect is more subtle, with 55% of these loci showing increased accessibility after Dex treatment. The ATAC-seq findings are consistent with a model in which ER increases chromatin accessibility, allowing GR to bind new loci.

The Combination of E2 and Dex Cooperate to Regulate Gene Expression

We sought to determine how crosstalk between ER and GR at the genomic binding level affects gene expression. To analyze gene expression responses to E2, Dex, and the combination of E2 and Dex, we performed RNA-seq and analyzed differential gene expression. We identified 286 genes that were regulated by E2 alone (188 upregulated and 98 downregulated) and 128 genes significantly regulated by Dex alone (120 upregulated and 8 downregulated). There was little overlap in the genes that were regulated by both E2 and Dex individual treatments with 24 overlapping genes that go in the same direction (19% of all Dex-regulated genes) and 6 overlapping genes that are regulated in opposite directions (5% of all Dex-regulated genes) (Figure S5A). *PR*, which is growth inhibitory in the uterus, is an example of an independent gene that is unaffected by Dex and induced by E2 and the combination treatment to a similar level. We examined other growth-inhibitory genes, including *EIG121*, *RALDH2*, *SFRP1*, and *SFRP4* (Deng et al., 2010; Westin et al., 2009), and found that each gene exhibited low expression in Ishikawa cells.

Upon treatment with both E2 and Dex, 371 genes were affected significantly (240 upregulated and 131 downregulated), and the combination treatment samples appeared to be more similar to the E2-treated samples. Most E2-induced gene expression changes were observed with the combination treatment (69%, Figure S5B), whereas fewer than half of the Dex-induced expression changes were seen with the combination treatment (43%, Figure S5C). This relationship is clear when analyzing principal components (Figure 6A). The overall pattern of gene expression upon E2 and Dex treatment suggests that E2 dominates the combination treatment, which explains the pro-growth phenotype, but Dex contributes by expanding the genes affected. The genes unique to the double induction are enriched in downregulation of cell-cell adherens junctions (adjusted p = 0.001, DAVID [Jiao et al., 2012]), including alpha-catenin (Knudsen et al., 1995), vinculin (Carisey and Ballestrem, 2011), and cingulin (Citi et al., 1988) (Figures S5D–S5F). The downregulation of cell adhesion proteins could partially explain the aggressiveness of ER- and GR-expressing tumors (Figure 1C). The genes uniquely regulated by the combination treatment are found near genomic loci bound by ER and GR after the double induction. GR double-induction sites are significantly closer to the Dex + E2-specific genes than are single-induction GR sites (Figure S5G; $p = 4.811 \times 10^{-4}$, Wilcoxon). ER double-induction sites are closer to Dex + E2-specific genes, but the effect is more subtle and the p value is marginal (Figure S5H, p = 0.0421, Wilcoxon). These findings are consistent with a shift in GR sites upon double induction, leading to novel regulation in cells co-treated with E2 and Dex.

For the 525 genes that exhibited differential gene expression in any treatment compared to controls, we performed regression analysis to look for genes that have a significant E2:Dex interaction term. We identified 112 genes with significant interaction terms; 21 genes had

higher expression in the double induction than expected based on the single inductions and 91 genes had lower than expected expression in the double induction. Of the genes with lower than expected double-induction expression, 61 (67%) were affected more by Dex alone than E2 alone, indicating a loss of Dex responsiveness that is consistent with altered GR binding. Figure 6B shows the expression of *HIF3A* and *PDGFB* as examples. Both *HIF3A* and *PDGFB* have regulatory loci nearby that exhibit less ATAC-seq signal upon E2 treatment as well as less GR binding after the double induction (Figures S6A and S6B). Of the genes with higher than expected double-induction expression, 62% were affected more by E2 alone than Dex alone, suggesting that GR may be assisting ER in regulating some genes. The examples of *SALL1* and *BAG3* are shown in Figure 6B. The intron of *BAG3* exhibits increased ER binding with the double induction, and a *SALL1* downstream site is only bound by GR upon treatment with both E2 and Dex (Figures S6C and S6D). Our results indicate that ER and GR can influence each other's ability to regulate gene expression through both increasing and decreasing genomic binding.

Many Genes Regulated by Dex and E2 Are Differentially Expressed in Endometrial Tumors

To determine whether the gene expression changes we observed in Ishikawa cells are observed in patient tumors, we analyzed gene expression from the endometrioid histology endometrial tumors in the TCGA cohort. We first categorized tumors as having high or low mRNA expression of ER and GR. Then, for each gene we compared gene expression in the GR high-ER high tumors to all of the other tumors. Of the genes that are differentially expressed when treated with the combination of Dex and E2 in Ishikawa cells, 37% were differentially expressed in the GR high-ER high tumors, which represents a highly significant overlap ($p = 1.285 \times 10^{-6}$, Fisher's exact test). Several examples of these genes are shown in Figure S7, which includes alpha-catenin (discussed above). We also found that nine of these genes exhibit expression that is associated with disease-free survival in endometrial cancer (Figure S7; *LMCD1* not shown because of space restrictions). These findings show that many of the genes uniquely regulated by Dex and E2 in Ishikawa cells are differentially expressed in GR high-ER high endometrial tumors, indicating that ER and GR are likely to exhibit molecular crosstalk in patients' tumors.

DISCUSSION

ER and GR play opposite phenotypic roles in the normal endometrium, with ER promoting growth and GR inhibiting growth. Here, we show that in endometrial cancer, GR expression is associated with worse outcomes and higher-grade tumors, and this association is observed only in the context of high ER expression. These findings seem to contradict the antigrowth effects of corticosteroids; however, our results show that growth inhibition is no longer observed after estrogen-induced hyperplasia has formed *in vivo* and that Dex, in combination with E2, promotes endometrial cancer cell growth in culture.

One possible explanation for the difference in GR-induced growth effects is that ER and GR are expressed in different compartments of the endometrium, with GR expressed in stromal cells and ER expressed in endometrial glands (Bamberger et al., 2001). GR signaling in stromal cells, through either auto-crine or paracrine changes, causes growth inhibition of the

normal uterus. However, GR activity in hyperplastic or cancerous endometrial cells, when co-expressed in the same cells as ER, no longer inhibits growth and may lead to more aggressive tumors. In fact, gene expression profiling of cells induced with both Dex and E2 uncovered a downregulation of cell adherence genes, which has the potential to cause a more metastatic phenotype. These findings are consistent with work in breast cancer that showed that GR-expressing tumors differentially regulate cell adhesion genes (Pan et al., 2011). Our findings indicate that the administration of Dex during treatment of endometrioid histology endometrial cancer should be re-evaluated.

Molecular characterization of ER and GR crosstalk in endometrial cancer cells revealed that ER is the dominant steroid hormone receptor in this setting. ER genomic binding is mostly unaffected by the activation of GR. In contrast, more than one-third of GR binding is altered by the activation of ER. It also appears that recruitment of GR to ER-bound sites has a functional consequence because it likely leads to an increase in regulatory activity as measured by H3K27ac and proximity to regulated genes. ER dominance is the opposite pattern that is observed in breast cancer cells, in which GR is dominant in dictating ER binding (Miranda et al., 2013). It is interesting that the difference in dominance between GR and ER is associated with differences in prognosis. GR is dominant over ER in breast cancer cells, resulting in a better prognosis when both are expressed (Pan et al., 2011), whereas ER is dominant over GR in endometrial cancer cells, resulting in a worse prognosis when both are expressed (Figure 1C). This leads to a model in which GR is generally growth inhibitory, ER is generally growth promoting, and the dominant factor dictates the aggressiveness of the tumor. It is unclear why ER is dominant in one setting and GR is dominant in another, but the possibility of differences in co-factor abundance is interesting.

To explore how ER was altering GR genomic binding, we used ATAC-seq to identify changes in chromatin accessibility. We found that the majority of GR-binding sites that are gained upon treatment with both Dex and E2 exhibit increased chromatin accessibility after E2 induction. These results are consistent with ER assisting in loading GR onto genomic loci, which is similar to breast cancer cells, in which GR assists in loading ER onto genomic loci (Miranda et al., 2013). We attempted co-immunoprecipitation of ER and GR and were unable to pull down one factor with an antibody that recognizes the other factor (data not shown), suggesting that ER and GR are not forming heterodimers and further supporting the model that crosstalk between ER and GR is occurring through alteration of each other’s chromatin interactions.

The genomic binding crosstalk between ER and GR has gene expression consequences. When endometrial cancer cells were induced with either Dex or E2 in isolation, there was little overlap in the genes affected. When cells were treated with both Dex and E2, the transcriptional response had greater similarity to an E2 response but with additional genes changing expression, including a downregulation of cell-cell adherens junction genes. A significant fraction of these additional genes are differentially expressed in ER high-GR high endometrial tumors, indicating that many genes are regulated by the combination of ER and GR generally in endometrial cancer. Unlike a recent report in breast cancer (Yang et al., 2017), GR does not appear to repress an E2 transcriptional response in endometrial cancer cells. Overall, approximately one-fifth of genes affected by any treatment exhibited an

unexpected gene expression level after double induction as determined by significant interaction terms in a linear model. Taken together, our findings are consistent with ER altering the genomic actions of GR, in which GR switches from regulating a distinct set of genes to promoting and enhancing an E2-driven transcriptional program in endometrial cells.

EXPERIMENTAL PROCEDURES

TCGA Data Analysis

RNA-seq and clinical data were downloaded from the TCGA data portal in December 2015. Gene expression measurements were taken from the level 3 RNaseqV2 normalized RSEM data. Only samples with endometrioid histology were analyzed for survival analysis. Cox regression to evaluate the association between gene expression and progression-free survival was performed in R (R Foundation) using binary classification of high and low expression for each steroid hormone receptor. For each steroid hormone receptor, we tried each decade percentile increment between the 20th and the 80th percentile to identify the cutoff between high and low expression that gave the most significant association with disease-free survival. The following cutoffs were used for each gene: GR, top 30th percentile was labeled high; ER, top 60th percentile; PR, top 80th percentile; AR, top 20th percentile; mineralocorticoid receptor, top 60th percentile; and estrogen receptor β, top 60th percentile. To identify genes that are differentially expressed in GR high-ER high tumors, we used a median cutoff for each gene to classify tumors as high or low. We then performed a Wilcoxon rank sum test to compare the expression in GR high-ER high tumors to all of the other endometrioid histology tumors.

IHC

Immunohistochemical staining of formalin-fixed paraffin slides was performed by ARUP Laboratories. In brief, 4- to 5-μm-thick tissue sections were prepared. The slides were placed on the automated immunostainer and de-paraffinized with the EZ Prep solution. The slides were then treated with CC1 (Cell Conditioning 1, pH 8.5) for 68 min at 95°C. The primary antibody against GR (clone D6H2L, #12041, Cell Signaling) was applied for 1 hr at a dilution of 1:100 at 35°C. Following removal of the primary antibody, the secondary antibody (goat anti-rabbit immunoglobulin [Ig]G, # B8895, Sigma-Aldrich) was applied for 1 hr at a dilution of 1:100 at 37°C. These slices were then exposed to the IView DAB Map detection kit (Ventana) and counterstained with hematoxylin for 8 min. Slides were removed from the autostainer and placed in a dH2O/Dawn mixture, and then dehydrated in graded alcohol. After dipping each slide 10 times in four changes of xylene, coverslips were put on and slides were read by board-certified pathologists. For patient samples, each patient consented under a protocol approved by the institutional review board of the University of Utah. All of the participants were female patients and age information was not analyzed for these patients.

Animal Studies

A total of thirty-five 8-week-old female BALB/c mice were used in this study. To induce estrogen-driven endometrial hyperplasia, E2 pellets were prepared and surgically implanted

into mice (n = 21), as previously described (Yang et al., 2015). Following 10 weeks of E2 exposure, mice were divided into three treatment arms to receive Dex, PBS, and 5% ethanol (n = 7 per arm). Fourteen mice did not receive E2 pellet implants and were divided into two groups for administration of Dex and PBS (n = 7 per group). Dex was dissolved in 5% ethanol and administered through intraperitoneal injection at a dose of 1 mg/kg and a frequency of 5 days on, 2 days off for a total of 21 days. Animals were sacrificed upon reaching the primary study endpoint on day 22 and necropsy including tissue harvesting ensued. Uteri were examined grossly and uterine weights were measured. Tissues were processed into formalin-fixed paraffin-embedded (FFPE) blocks and stained with H&E for histopathological analysis. Animals were housed in the animal facility of the Comparative Medicine Center at the University of Utah under standard conditions. All of the procedures conducted were approved by the Institutional Animal Care and Use Committee of the University of Utah.

Cell Culture

Ishikawa cells (Sigma-Aldrich) were grown in RPMI-1640 with 10% fetal bovine serum and 50 U/mL penicillin and 50 mg/mL streptomycin. At least 4 days before induction, cells were moved to phenol-red free RPMI-1640 with 10% charcoal-dextran stripped fetal bovine serum to remove hormones. Cells were treated with DMSO, 10 nM E2, 100 nM Dex, or the combination of 10 nM E2 and 100 nM Dex for either 1 hr for ChIP-seq and ATAC-seq or 8 hr for RNA-seq.

3D Culture

Ishikawa cells were grown and transferred to hormone-depleted RPMI-1640, as described above. Cells were suspended in Matrigel (growth factor reduced, phenol-red free), and 500 cells were plated with 9 μL Matrigel and 500 μL media per well in a 48-well glass-bottom plate (MalTek, 48-mm glass bottom). Cells were treated with DMSO, 10 nM E2, 100 nM Dex, or the combination of 10 nM E2 and 100 nM Dex. Relative ATP levels were measured using CellTiter Glo 3D (Promega) after 14 days.

ChIP-Seq

After inductions, cells were crosslinked with 1% formaldehyde for 10 min at room temperature and then treated with 125 mM glycine for 5 min to stop crosslinking. Crosslinked cells were then washed with cold PBS and scraped to harvest. ChIP was performed as previously described (Reddy et al., 2009). Sonication was performed on an Active Motif EpiShear Probe Sonicator with 8 cycles of 30 s, with 30 s of rest, at 40% amplitude. The antibodies used were ER (Santa Cruz HC-20), GR (Santa Cruz E-20), and H3K27ac (Active Motif 39133). ChIP-seq reads for each treatment were compared to ChIP-seq libraries from control (DMSO) treated cells for the same factor (e.g., GR in Dex was compared to GR in DMSO). Reads were aligned to the hg19 build of the human genome using Bowtie with the following parameters: -m 1 -t–best -q -S -l 32 -e 80 -n 2. Peaks were called using Model-Based Analysis of ChIP-seq-2 (MACS2) (Zhang et al., 2008) with a p value cutoff of 1e—10 and the mfold parameter constrained between 15 and 100. Counts between sets were calculated using bedtools coverage (Quinlan and Hall, 2010) to find read depth at all sites covered by peaks called by MACS2. These data were combined using gawk

and examined and graphed using R. Motif finding was performed on 100 bp surrounding the top 500 peaks based on their integer score (column 5 of narrowPeak file). Motifs were discovered using the meme suite (Bailey et al., 2009), searching for motifs between 6 and 50 bases in length, with zero or one occurrence per sequence. We used Patser (Hertz and Stormo, 1999) to count the number of sites with significant full- and half-site EREs and GRBEs within 50 bp of the summit of each peak.

RNA-Seq

After inductions, cell lysates were harvested with buffer RLT Plus (QIAGEN) supplemented with 1% beta-mercaptoethanol and passed through a 21G needle to shear genomic DNA. RNA was purified using RNA clean and concentrator with the optional DNase treatment (Zymo Research). Poly(A)-selected RNA-seq libraries were constructed with the KAPA Stranded mRNA-seq kit (Kapa Biosystems) using 1 mg total RNA. Sequencing reads were aligned to the hg19 build of the human genome using HISAT2 (Kim et al., 2015). Sequence alignment map (SAM) files were converted to binary sequence alignment map (BAM) format and sorted using samtools (Li et al., 2009). Reads mapping to genes were counted using featureCounts from the SubRead package (Liao et al., 2014). Reads were normalized and differential analysis was conducted in a pairwise manner using DESeq2 (Love et al., 2014). Genes were considered significant if they had an adjusted p value of ≤0.1. To find significant E2:Dex interaction terms, we constructed linear models in R using the linear model function and looked for E2:Dex coefficients that were significantly different from zero with a p value < 0.05.

ATAC-Seq

ATAC-seq was performed on 250,000 cells for each library (described by Buenrostro et al., 2013). Tn5 transposase, with Illumina adapters, was constructed as outlined earlier (Picelli et al., 2014). Sequencing reads were aligned to hg19 using Bowtie (Langmead et al., 2009) with the following parameters: -m 1 -t–best -q -S -l 32 -e 80 -n 2. SAM files were converted to BAM files and sorted using samtools (Li et al., 2009). MACS2 (Zhang et al., 2008) was used to call peaks without a control input. We used a cutoff p value of 1e—10 when calling peaks. featureCounts (Liao et al., 2014) was used to quantify reads that aligned in regions ± 250 bp from ER-or GR-binding site summits from the ChIP-seq experiments. These reads were then normalized and differential expression was determined by comparing samples in a pairwise manner using the DESeq2 package for R (Love et al., 2014).

Statistical Analysis

All of the statistical analyses were performed in R version 3.4.0, with the exception of the p value calculated by DAVID, and the statistical test used for each analysis is listed next to the reported p value. The R functions used were wilcox.test, t.test, fisher.test, and coxph (from the package survival).

Supplementary Material

Refer to Web version on PubMed Central for supplementary material.

Acknowledgments

This work was supported by NIH/National Human Genome Research Institute (NHGRI) R00 HG006922 and NIH/NHGRI R01 HG008974 (to J.G.), the Huntsman Cancer Institute, and the Women's Cancers Disease-Oriented Team at the Huntsman Cancer Institute. Research reported in this publication utilized the High-Throughput Genomics Shared Resource at the University of Utah and was supported by NIH/National Cancer Institute award P30 CA042014. A.C.R. was supported by diversity supplement R00 HG006922S1. We thank Ed Grow for providing reagents and we thank K.-T. Varley as well as Gertz and Varley laboratory members for their helpful comments on the study and the manuscript.

References

Arora VK, Schenkein E, Murali R, Subudhi SK, Wongvipat J, Balbas MD, Shah N, Cai L, Efstathiou E, Logothetis C, et al. Glucocorticoid receptor confers resistance to antiandrogens by bypassing androgen receptor blockade. Cell. 2013; 155:1309–1322. [PubMed: 24315100]

Backes FJ, Walker CJ, Goodfellow PJ, Hade EM, Agarwal G, Mutch D, Cohn DE, Suarez AA. Estrogen receptor-alpha as a predictive biomarker in endometrioid endometrial cancer. Gynecol Oncol. 2016; 141:312–317. [PubMed: 26957478]

Bailey TL, Boden M, Buske FA, Frith M, Grant CE, Clementi L, Ren J, Li WW, Noble WS. MEME SUITE: tools for motif discovery and searching. Nucleic Acids Res. 2009; 37:W202–W208. [PubMed: 19458158]

Bamberger AM, Milde-Langosch K, Löning T, Bamberger CM. The glucocorticoid receptor is specifically expressed in the stromal compartment of the human endometrium. J Clin Endocrinol Metab. 2001; 86:5071–5074. [PubMed: 11600587]

Bever AT, Hisaw FL, Velardo JT. Inhibitory action of desoxycorticosterone acetate, cortisone acetate, and testosterone on uterine growth induced by estradiol-17beta. Endocrinology. 1956; 59:165–169. [PubMed: 13356781]

Bitman J, Cecil HC. Differential inhibition by cortisol of estrogen-stimulated uterine responses. Endocrinology. 1967; 80:423–429. [PubMed: 5227344]

Bolt MJ, Stossi F, Newberg JY, Orjalo A, Johansson HE, Mancini MA. Coactivators enable glucocorticoid receptor recruitment to fine-tune estrogen receptor transcriptional responses. Nucleic Acids Res. 2013; 41:4036–4048. [PubMed: 23444138]

Buenrostro JD, Giresi PG, Zaba LC, Chang HY, Greenleaf WJ. Transposition of native chromatin for fast and sensitive epigenomic profiling of open chromatin, DNA-binding proteins and nucleosome position. Nat Methods. 2013; 10:1213–1218. [PubMed: 24097267]

Carisey A, Ballestrem C. Vinculin, an adapter protein in control of cell adhesion signalling. Eur J Cell Biol. 2011; 90:157–163. [PubMed: 20655620]

Citi S, Sabanay H, Jakes R, Geiger B, Kendrick-Jones J. Cingulin, a new peripheral component of tight junctions. Nature. 1988; 333:272–276. [PubMed: 3285223]

D'Amato NC, Gordon MA, Babbs B, Spoelstra NS, Carson Butterfield KT, Torkko KC, Phan VT, Barton VN, Rogers TJ, Sartorius CA, et al. Cooperative dynamics of AR and ER activity in breast cancer. Mol Cancer Res. 2016; 14:1054–1067. [PubMed: 27565181]

Deng L, Feng J, Broaddus RR. The novel estrogen-induced gene EIG121 regulates autophagy and promotes cell survival under stress. Cell Death Dis. 2010; 1:e32. [PubMed: 21072319]

Gunin AG, Mashin IN, Zakharov DA. Proliferation, mitosis orientation and morphogenetic changes in the uterus of mice following chronic treatment with both estrogen and glucocorticoid hormones. J Endocrinol. 2001; 169:23–31. [PubMed: 11250643]

Haynes LE, Lendon CL, Barber DJ, Mitchell IJ. 17 Beta-oestradiol attenuates dexamethasone-induced lethal and sublethal neuronal damage in the striatum and hippocampus. Neuroscience. 2003; 120:799–806. [PubMed: 12895519]

Hertz GZ, Stormo GD. Identifying DNA and protein patterns with statistically significant alignments of multiple sequences. Bioinformatics. 1999; 15:563–577. [PubMed: 10487864]

Isikbay M, Otto K, Kregel S, Kach J, Cai Y, Vander Griend DJ, Conzen SD, Szmulewitz RZ. Glucocorticoid receptor activity contributes to resistance to androgen-targeted therapy in prostate cancer. Horm Cancer. 2014; 5:72–89. [PubMed: 24615402]

Jiao X, Sherman BT, Huang W, Stephens R, Baseler MW, Lane HC, Lempicki RA. DAVID-WS: a stateful web service to facilitate gene/ protein list analysis. Bioinformatics. 2012; 28:1805–1806. [PubMed: 22543366]

Jozwik KM, Carroll JS. Pioneer factors in hormone-dependent cancers. Nat Rev Cancer. 2012; 12:381–385. [PubMed: 22555282]

Kandoth C, Schultz N, Cherniack AD, Akbani R, Liu Y, Shen H, Robertson AG, Pashtan I, Shen R, Benz CC, et al. Integrated genomic characterization of endometrial carcinoma. Nature. 2013; 497:67–73. [PubMed: 23636398]

Karmakar S, Jin Y, Nagaich AK. Interaction of glucocorticoid receptor (GR) with estrogen receptor (ER) α and activator protein 1 (AP1) in dexamethasone-mediated interference of ERα activity. J Biol Chem. 2013; 288:24020–24034. [PubMed: 23814048]

Kim D, Langmead B, Salzberg SL. HISAT: a fast spliced aligner with low memory requirements. Nat Methods. 2015; 12:357–360. [PubMed: 25751142]

Knudsen KA, Soler AP, Johnson KR, Wheelock MJ. Interaction of alpha-actinin with the cadherin/ catenin cell-cell adhesion complex via alpha-catenin. J Cell Biol. 1995; 130:67–77. [PubMed: 7790378]

Lam KS, Lee MF, Tam SP, Srivastava G. Gene expression of the receptor for growth-hormone-releasing hormone is physiologically regulated by glucocorticoids and estrogen. Neuroendocrinology. 1996; 63:475–480. [PubMed: 8793888]

Langmead B, Trapnell C, Pop M, Salzberg SL. Ultrafast and memory-efficient alignment of short DNA sequences to the human genome. Genome Biol. 2009; 10:R25. [PubMed: 19261174]

Li H, Handsaker B, Wysoker A, Fennell T, Ruan J, Homer N, Marth G, Abecasis G, Durbin R, 1000 Genome Project Data Processing Subgroup. The sequence alignment/map format and SAMtools. Bioinformatics. 2009; 25:2078–2079. [PubMed: 19505943]

Li J, Alyamani M, Zhang A, Chang KH, Berk M, Li Z, Zhu Z, Petro M, Magi-Galluzzi C, Taplin ME, et al. Aberrant corticosteroid metabolism in tumor cells enables GR takeover in enzalutamide resistant prostate cancer. eLife. 2017; 6:e20183. [PubMed: 28191869]

Liao Y, Smyth GK, Shi W. featureCounts: an efficient general purpose program for assigning sequence reads to genomic features. Bioinformatics. 2014; 30:923–930. [PubMed: 24227677]

Love MI, Huber W, Anders S. Moderated estimation of fold change and dispersion for RNA-seq data with DESeq2. Genome Biol. 2014; 15:550. [PubMed: 25516281]

Markaverich BM, Upchurch S, Clark JH. Progesterone and dexamethasone antagonism of uterine growth: a role for a second nuclear binding site for estradiol in estrogen action. J Steroid Biochem. 1981; 14:125–132. [PubMed: 7206703]

Meyer ME, Gronemeyer H, Turcotte B, Bocquel MT, Tasset D, Chambon P. Steroid hormone receptors compete for factors that mediate their enhancer function. Cell. 1989; 57:433–442. [PubMed: 2720778]

Miranda TB, Voss TC, Sung MH, Baek S, John S, Hawkins M, Grøntved L, Schiltz RL, Hager GL. Reprogramming the chromatin landscape: interplay of the estrogen and glucocorticoid receptors at the genomic level. Cancer Res. 2013; 73:5130–5139. [PubMed: 23803465]

Mohammed H, Russell IA, Stark R, Rueda OM, Hickey TE, Tarulli GA, Serandour AA, Birrell SN, Bruna A, Saadi A, et al. Progesterone receptor modulates ERα action in breast cancer. Nature. 2015; 523:313–317. [PubMed: 26153859]

Pan D, Kocherginsky M, Conzen SD. Activation of the glucocorticoid receptor is associated with poor prognosis in estrogen receptor-negative breast cancer. Cancer Res. 2011; 71:6360–6370. [PubMed: 21868756]

Picelli S, Björklund AK, Reinius B, Sagasser S, Winberg G, Sandberg R. Tn5 transposase and tagmentation procedures for massively scaled sequencing projects. Genome Res. 2014; 24:2033–2040. [PubMed: 25079858]

Quinlan AR, Hall IM. BEDTools: a flexible suite of utilities for comparing genomic features. Bioinformatics. 2010; 26:841–842. [PubMed: 20110278]

Rabin DS, Johnson EO, Brandon DD, Liapi C, Chrousos GP. Glucocorticoids inhibit estradiol-mediated uterine growth: possible role of the uterine estradiol receptor. Biol Reprod. 1990; 42:74–80. [PubMed: 2310819]

Reddy TE, Pauli F, Sprouse RO, Neff NF, Newberry KM, Garabedian MJ, Myers RM. Genomic determination of the glucocorticoid response reveals unexpected mechanisms of gene regulation. Genome Res. 2009; 19:2163–2171. [PubMed: 19801529]

Rhen T, Grissom S, Afshari C, Cidlowski JA. Dexamethasone blocks the rapid biological effects of 17beta-estradiol in the rat uterus without antagonizing its global genomic actions. FASEB J. 2003; 17:1849–1870. [PubMed: 14519664]

Robinson JLL, Macarthur S, Ross-Innes CS, Tilley WD, Neal DE, Mills IG, Carroll JS. Androgen receptor driven transcription in molecular apocrine breast cancer is mediated by FoxA1. EMBO J. 2011; 30:3019–3027. [PubMed: 21701558]

Saso S, Chatterjee J, Georgiou E, Ditri AM, Smith JR, Ghaem-Maghami S. Endometrial cancer. BMJ. 2011; 343:d3954. [PubMed: 21734165]

Singhal H, Greene ME, Tarulli G, Zarnke AL, Bourgo RJ, Laine M, Chang YF, Ma S, Dembo AG, Raj GV, et al. Genomic agonism and phenotypic antagonism between estrogen and progesterone receptors in breast cancer. Sci Adv. 2016; 2:e1501924. [PubMed: 27386569]

Tangen IL, Werner HM, Berg A, Halle MK, Kusonmano K, Trovik J, Hoivik EA, Mills GB, Krakstad C, Salvesen HB. Loss of progesterone receptor links to high proliferation and increases from primary to metastatic endometrial cancer lesions. Eur J Cancer. 2014; 50:3003–3010. [PubMed: 25281525]

Terakawa N, Shimizu I, Aono T, Tanizawa O, Matsumoto K. Dexamethasone suppresses estrogen action at the pituitary level without modulating estrogen receptor dynamics. J Steroid Biochem. 1985; 23:385–388. [PubMed: 4068700]

Voss TC, Schiltz RL, Sung MH, Yen PM, Stamatoyannopoulos JA, Biddie SC, Johnson TA, Miranda TB, John S, Hager GL. Dynamic exchange at regulatory elements during chromatin remodeling underlies assisted loading mechanism. Cell. 2011; 146:544–554. [PubMed: 21835447]

Westin SN, Broaddus RR, Deng L, McCampbell A, Lu KH, Lacour RA, Milam MR, Urbauer DL, Mueller P, Pickar JH, Loose DS. Molecular clustering of endometrial carcinoma based on estrogen-induced gene expression. Cancer Biol Ther. 2009; 8:2126–2135. [PubMed: 19755863]

Wik E, Ræder MB, Krakstad C, Trovik J, Birkeland E, Hoivik EA, Mjos S, Werner HM, Mannelqvist M, Stefansson IM, et al. Lack of estrogen receptor-α is associated with epithelial-mesenchymal transition and PI3K alterations in endometrial carcinoma. Clin Cancer Res. 2013; 19:1094–1105. [PubMed: 23319822]

Yang CH, Almomen A, Wee YS, Jarboe EA, Peterson CM, Janát-Amsbury MM. An estrogen-induced endometrial hyperplasia mouse model recapitulating human disease progression and genetic aberrations. Cancer Med. 2015; 4:1039–1050. [PubMed: 25809780]

Yang F, Ma Q, Liu Z, Li W, Tan Y, Jin C, Ma W, Hu Y, Shen J, Ohgi KA, et al. Glucocorticoid receptor:MegaTrans switching mediates the repression of an ERα-regulated transcriptional program. Mol Cell. 2017; 66:321–331.e6. [PubMed: 28475868]

Zhang Y, Liu T, Meyer CA, Eeckhoute J, Johnson DS, Bernstein BE, Nusbaum C, Myers RM, Brown M, Li W, Liu XS. Model-based analysis of ChIP-Seq (MACS). Genome Biol. 2008; 9:R137. [PubMed: 18798982]

Zhou F, Bouillard B, Pharaboz-Joly MO, André J. Non-classical antiestrogenic actions of dexamethasone in variant MCF-7 human breast cancer cells in culture. Mol Cell Endocrinol. 1989; 66:189–197. [PubMed: 2612731]

Highlights

- GR expression is associated with poor prognosis in ER expressing endometrial tumors
- Dexamethasone inhibits normal uterine growth, but not estradiol-induced hyperplasia
- Co-stimulus of ER and GR causes GR to bind ER-bound loc that are more accessible
- Co-stimulus response is similar to estradiol only with some unique regulated genes

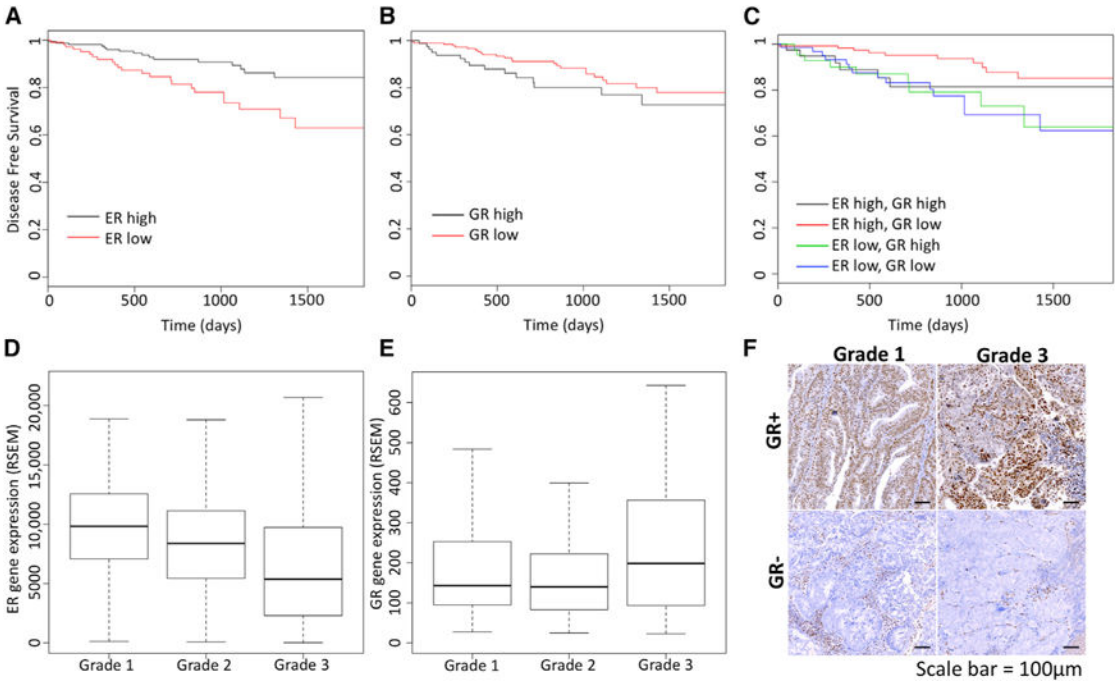

Figure 1. GR Expression Is Associated with Poor Prognosis in Endometrioid Endometrial Cancer

(A–E) Kaplan-Meier curves show the association of disease-free survival with estrogen receptor α (ER) expression (A, high is top 60% tumors), glucocorticoid receptor (GR) expression (B, high is top 30% tumors), and the combination (C). Higher ER expression is associated with better prognosis, whereas higher GR expression is associated with worse outcomes, but only in the context of high ER expression. ER expression is negatively correlated with tumor grade (D), and GR expression is positively correlated with tumor grade (E).

(F) Examples of GR immunohistochemistry staining are shown for grade 1 and grade 3 tumors.

Scale bar represents 100 μm.

See also Figures S1 and S2.

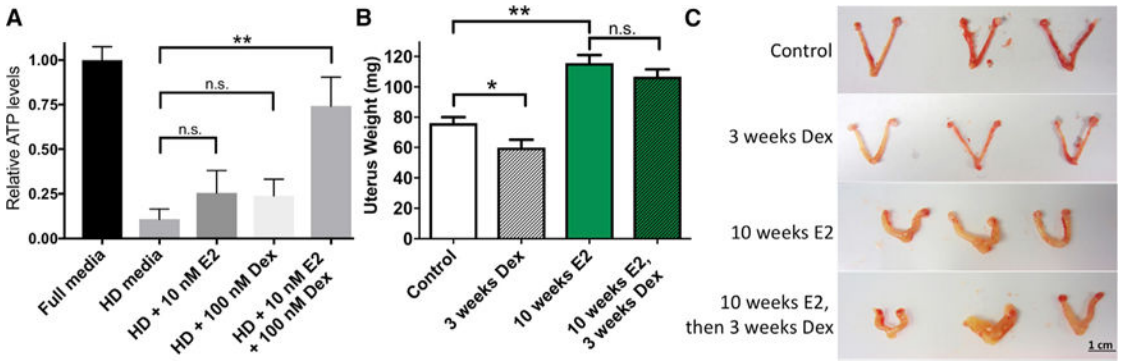

Figure 2. Growth Effects of Dexamethasone Are Influenced by 17β-Estradiol (E2)

(A) Hormone-depleted (HD) media reduces growth of Ishikawa cells, as measured by relative ATP levels. The addition of E2 or Dexamethasone (Dex) to HD media modestly increases growth, and the combination of E2 and Dex restores growth to levels similar to those of full media. Data are represented as means ± SEMs.

(B) Uterine weight is reduced by Dex in mice. Continuous E2 exposure for 10 weeks significantly increases uterine weight, and subsequent addition of Dex does not significantly reduce this effect. Data are represented as means ± SEMs.

(C) Examples of uteri from the categories in (B). Scale bar represents 1 cm.

*$p < 0.05$; **$p < 0.01$; n.s. = not significant ($p > 0.05$). See also Figure S3.

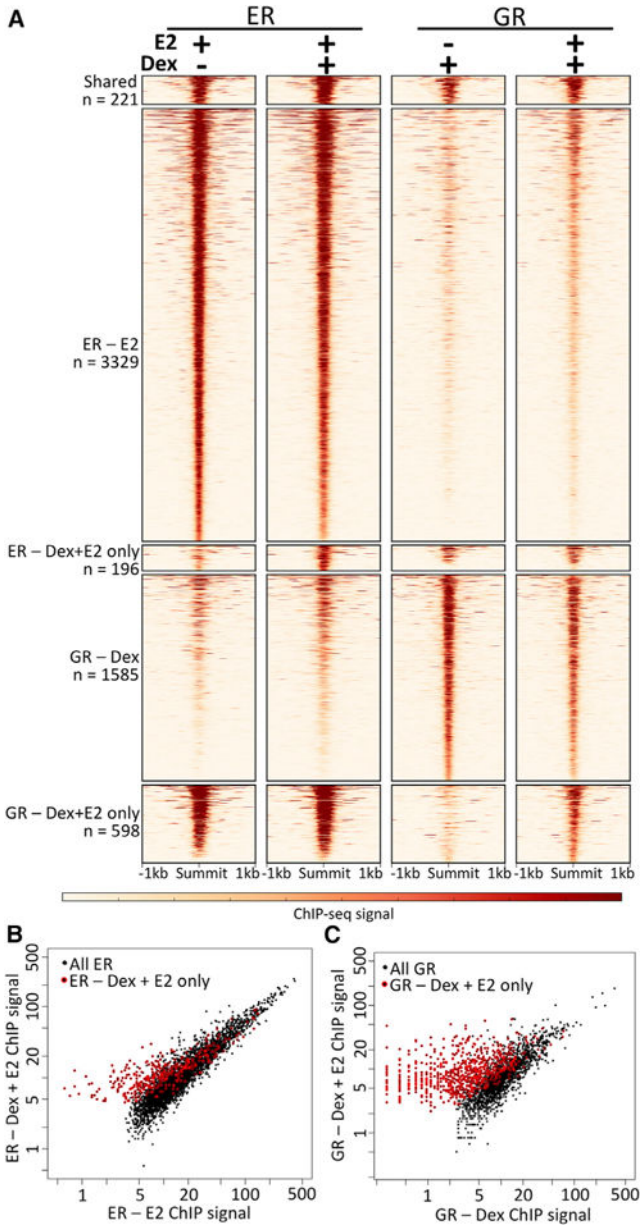

Figure 3. E2 Alters Genomic Binding

(A) Heatmaps of chromatin immunoprecipitation sequencing (ChIP-seq) signal of ER and GR after single and double inductions show that there is a unique set of sites where GR binds only after double induction.

(B and C) ChIP-seq signal is plotted for each ER (B) and GR (C) binding site comparing single induction (x axis) and double induction (y axis). Sites unique to the double induction are shown in red, with GR double-induction sites showing markedly different signals. Signal is displayed as reads per million. See also Figure S4.

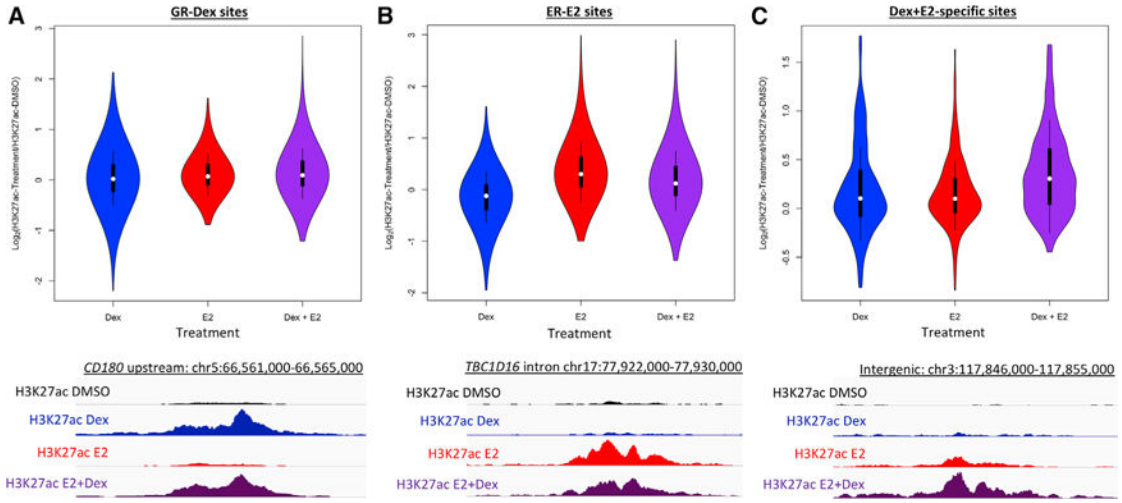

Figure 4. Histone Acetylation Is Increased at ER- and GR-Bound Sites Upon Double Induction

(A–C) For GR sites bound after Dex-only treatment (A), ER sites bound after E2-only treatment (B), and sites bound by both ER and GR after double induction (C), the distribution of relative levels of histone H3 lysine 27 (H3K27ac) for Dex (blue), E2 (red), and the combination of Dex and E2 (purple) compared to the vehicle control are shown. H3K27ac increases at loci bound by both ER and GR specifically after the combination treatment. Example loci for each type of site are shown in the bottom panels, with each track for a site shown on the same scale.

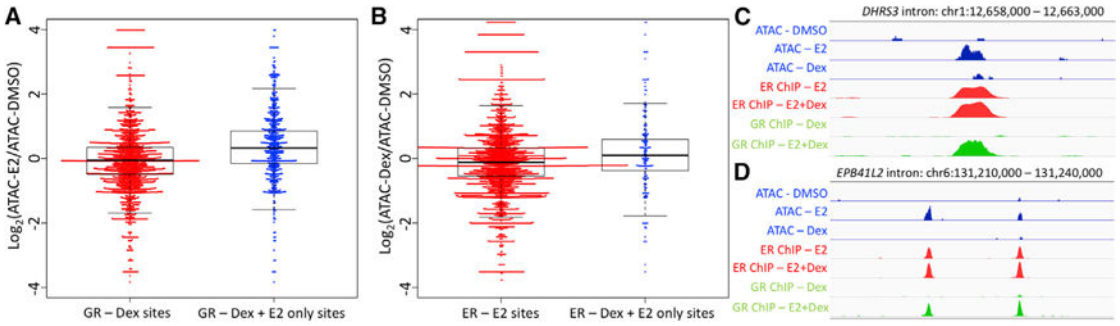

Figure 5. Chromatin Accessibility Is Increased at Double-Induction-Specific GR-Bound Sites

(A–D) The log ratio of assay for transposase-accessible chromatin using sequencing (ATAC-seq) signal after E2 treatment versus vehicle control (A) and Dex treatment versus vehicle controls (B) is shown for all (red) and double-induction-specific (blue) GR (A) and ER (B) sites. The ATAC-seq signal is increased upon E2 induction at GR sites only observed after E2 + Dex treatment. Signal tracks of ATAC-seq signal (blue), ER ChIP-seq signal (red), and GR ChIP-seq signal (green) are shown for loci nearby *DHRS3* (C) and *EPB4IL2* (D). Signal tracks of the same type are shown on the same scale.

See also Figure S6.

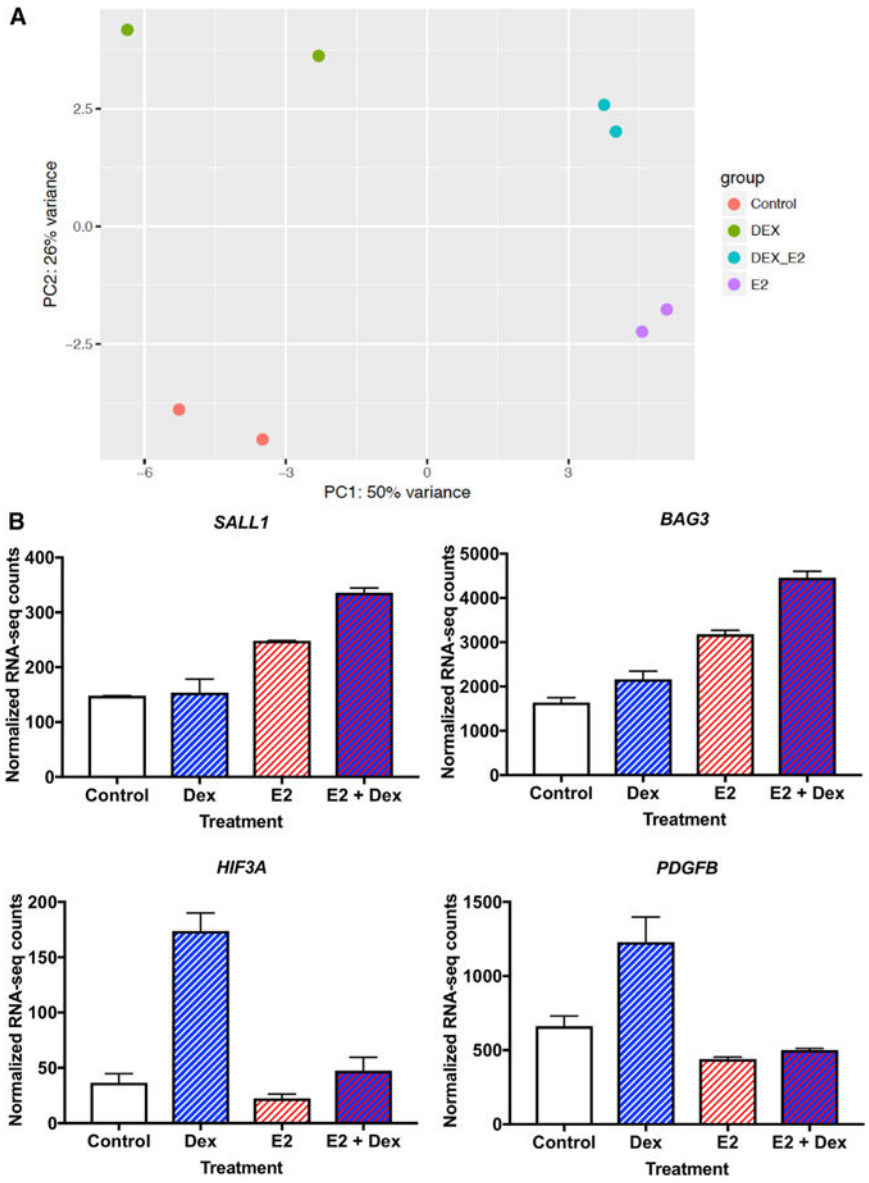

Figure 6. Gene Expression Consequences of Double Induction

(A) Principal-component analysis of RNA-seq from E2, Dex and the combination treatments, shows that E2 + Dex-treated samples (cyan) are more similar to E2-treated samples (purple) than are Dex-treated samples (green) or vehicle-treated samples (red).

(B) Examples of genes that exhibit unexpected gene expression levels upon double treatment are *SALL1*, *BAG3*, *HIF3A*, and *PDGFB*. Data are represented as means ± SEMs.

See also Figures S5 and S7.

Table 1

Motif Occurrences at ER- and GR-Bound Loci

	ER (%)		GR (%)	
Motif	**E2**	**Dex + E2 Only**	**Dex**	**Dex + E2 Only**
ERE full site	27	8	3	21
ERE half-site	91	76	55	82
GRBE full site	6	14	45	11
GRBE half-site	53	64	81	60

ERE, estrogen-response element; GRBE, glucocorticoid receptor-binding element.